ELSEVIER

Journal of Nuclear Materials 258–263 (1998) 719–723

journal of nuclear materials

Microstructural study of hydrogen-implanted beryllium

S.P. Vagin [a], P.V. Chakrov [a,*], B.D. Utkelbayev [a], L.A. Jacobson [b], R.D. Field [b], H. Kung [b]

[a] *Almaty branch of the Institute of Atomic Energy NNC RK, Ibragimova Str. 1, Almaty 480082, Kazakhstan*
[b] *Los Alamos National Laboratory, Los Alamos, NM 87545, USA*

Abstract

Hot pressed beryllium (TGP-56) was implanted by 650 keV H^+ ions to a dose of 6.7×10^{16} cm^{-2} at a temperature below 50°C. TEM examinations were performed both at as-irradiated specimens and after post-irradiation annealings at 400–600°C for 15 min. After irradiation, a high density of "black dot" defects with a size of about 5 nm is observed in the straggling zone, some of which are resolved as small dislocation loops. During post-irradiation annealing, growth of dislocation loops and oriented gas-filled bubbles are observed in the damaged zone. The bubbles are strongly elongated along the ⟨0 0 0 1⟩ direction, and their sidelong facts lie along {1-1 0 0} planes. These facets have a regular "toothed" surface with "tooth" facets on {1-1 0 0} planes. The size of the "teeth" increases with annealing temperature, as well as the total volume of bubbles, with their length growing faster than their width.

1. Introduction

Beryllium is planned to be used as a plasma facing material for the first wall of a fusion reactor due to its properties that lead to low plasma pollution and the ability to withstand intense thermal and radiation fluxes [1]. The behaviour of hydrogen isotopes in the material is one of the important scientific and engineering problems related to the design of the reactor [2–4]. The processes of retention and interaction of hydrogen isotopes in beryllium are presently being studied intensively [5–9]. Special interest is focused on obtaining data on the defect structure produced by hydrogen implantation, and on the determination of the state of hydrogen in the material, depending on the temperature and dose of irradiation.

The type of defect responsible for hydrogen trapping has been found to depend on irradiation temperature. At low temperatures these are monovacancies, small vacancy clusters, and presumably, amorphous regions of beryllium hydride [10]. At elevated temperatures hydrogen trapping into bubbles is observed [5–8,11]. However, there is a shortage of detailed information on the types of radiation defects, and on the mechanisms of hydrogen isotope trapping, desorption and permeability in beryllium. The present work is devoted to the study of defect structure in beryllium irradiated with 650 keV H^+ ions up to a dose of 6.7×10^{16} cm^{-2} at room temperature, and the evolution of this defect structure during post irradiation thermal annealing.

2. Experiment

Hot pressed beryllium (TGP-56 grade) was irradiated in the ion accelerator UKP 2-1 at the National Nuclear Center, Republic of Kazakstan (NNC RK) with 650 keV protons, at a temperature below 50°C and a beam current of 1 $\mu A/cm^2$, up to a dose of 6.7×10^{16} cm^{-2}. A technique was applied that allows the study of the whole range of the ion damaged zone by transmission electron microscopy (TEM). This technique consists of the depositing of a special serrated mask in front of the sample (shown schematically in Fig. 1). As a result of irradiation in the presence of mask, periodically arranged zones of damage, including hydrogen doped regions, are formed in the bulk of the sample. Further thinning by usual methods allows the observation of the

* Corresponding author. Tel.: +7 3272 690480; fax: +7 3272 608271; e-mail: root@iae.almaty.kz.

0022-3115/98/$19.00
PII: S 0 0 2 2 - 3 1 1 5 (9 8) 0 0 3 7 7 - 8

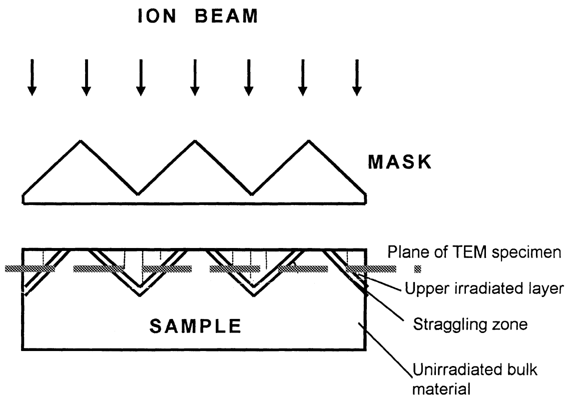

Fig. 1. Scheme of irradiation.

whole ion damaged zone in a single TEM specimen. Microstructural examinations were performed using transmission electron microscopes EM-125, Philips CM30 and JEOL 3000F. Thermal annealings of irradiated samples were carried out in a vacuum of 10^{-3} Pa for a period of 15 min at various temperatures.

3. Results

After irradiation, a high density of "black dot" defects with a size of about 5 nm is observed in the straggling zone (Fig. 2). The best contrast of these defects takes place at dynamic imaging conditions ($s \approx 0$). Weak beam images show strong stress fields around the defects, some of which are resolved as small dislocation loops. The width of the straggling zone is about 1000 nm, in agreement with its calculated value (TRIM). The calculated degree of damage varies from 7×10^{-3} to 7×10^{-2} dpa through the zone, and the calculated concentration of implanted hydrogen from 0.05 to 1.3 at.%. High resolution micrographs (such as presented at Fig. 3) show that some of the defects look like disordered (amorphous) regions. Such regions are only observed in the damage zone and in very thin areas of the sample, where the contribution of the surrounding crystal matrix to the image formation is small. Apart from disordered regions, unusual crystal regions about 3–6 nm in size are present in the zone of maximum hydrogen concentration. These crystal inclusions have a lattice parameter different from the beryllium HCP lattice and, in some occurrences, have a clear faceted hexagon shape.

During post-irradiation annealing, growth of dislocation loops (Fig. 4) and oriented cavities are observed in the straggling zone. The cavities are strongly elongated along the ⟨0 0 0 1⟩ direction, the value of their length/width ratio being up to 15 at 600°C (Fig. 5(a)). As was determined by stereo microscopic investigations in different zone axes, the sidelong facets of these cavities lie along {1–100} planes (Fig. 5(b)). However, they were found to have a fine structure. These facets have a regular "toothed" surface with "tooth" facets on 1–101 planes. The size of the "teeth" is about 10 nm at 500°C and about 20 nm at 600°C, and is not significantly dependent on the size of the cavity. Distinctive contrast at dynamic imaging conditions (Fig. 6) shows the stressed state of the matrix around the cavities, so they are assumed to be gas-filled bubbles. The total volume of bubbles increases with temperature, with their length growing faster than their width. In addition to the

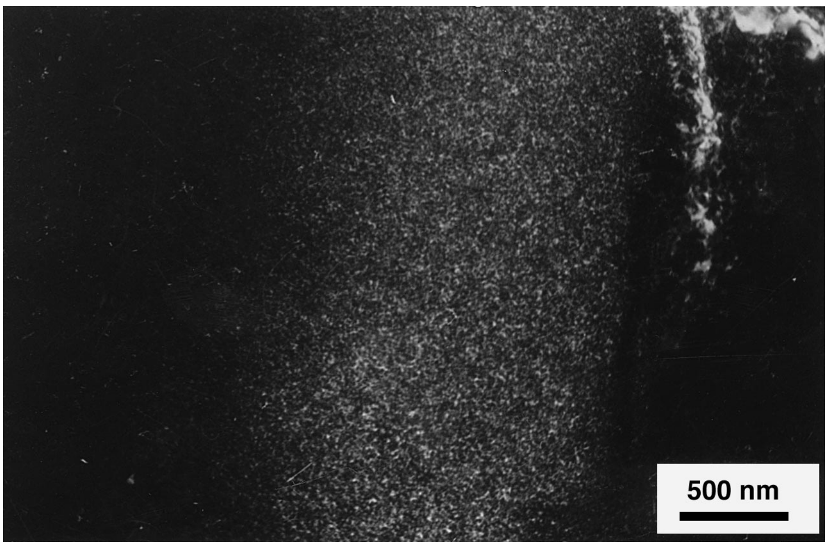

Fig. 2. Dark field micrograph of damaged zone in hydrogen-implanted beryllium (650 KeV, 6.7×10^{16} cm^{-2}).

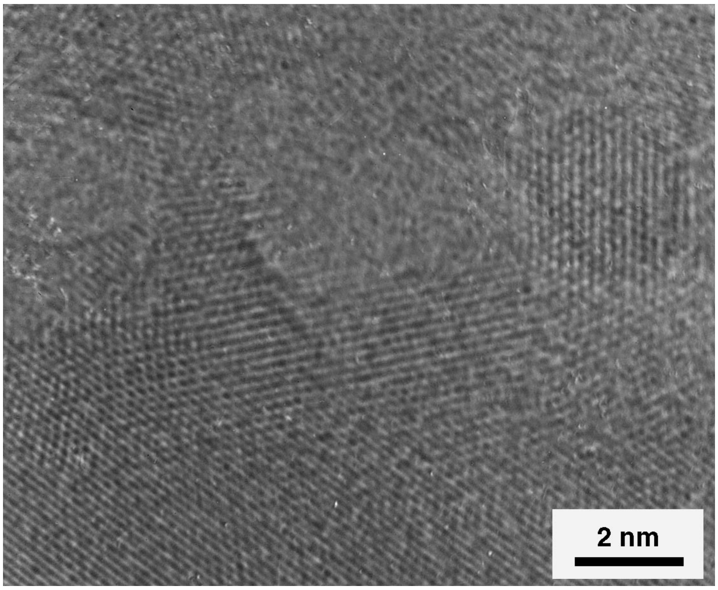

Fig. 3. High resolution TEM micrograph of the damaged zone in hydrogen-implanted beryllium.

bubbles, a high density of dislocations remains up to 600°C, and all bubbles are fixed on the dislocations (Fig. 7).

4. Discussion and conclusions

As has been observed in various metals irradiated at room temperature by low energy gaseous ions, an intense formation of fine cavities with high density is observed in spite of the low mobility of vacancies. Numerous studies have shown that these cavities are gas-filled bubbles. At higher doses such bubbles are arranged into an ordered lattice [12]. Similar bubbles were also observed in beryllium implanted with low energy D ions at doses of 3×10^{20} m^{-2} and higher [5,7,8]. In our experiment a high density of small disordered regions was found. These are caused, obviously, by cascade damage from the primary knock-ions with energy up to 230 keV. As was found in [13,14], at low doses of im-

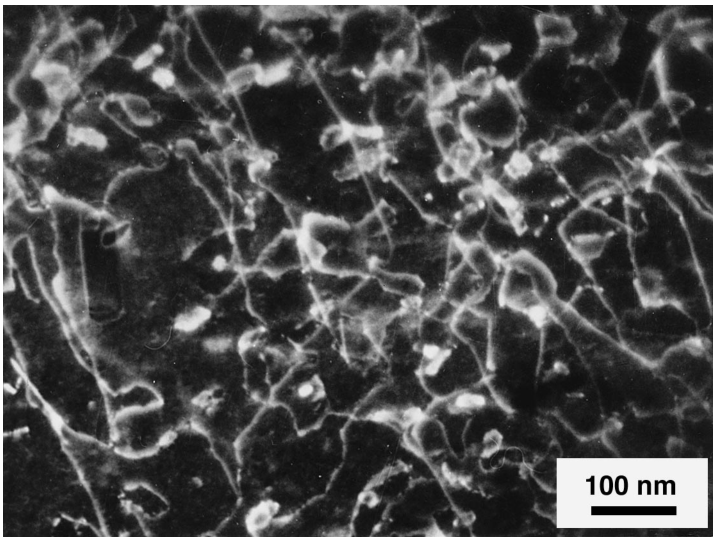

Fig. 4. Dislocation structure in the damaged zone after thermal annealing for 15 min at 200°C.

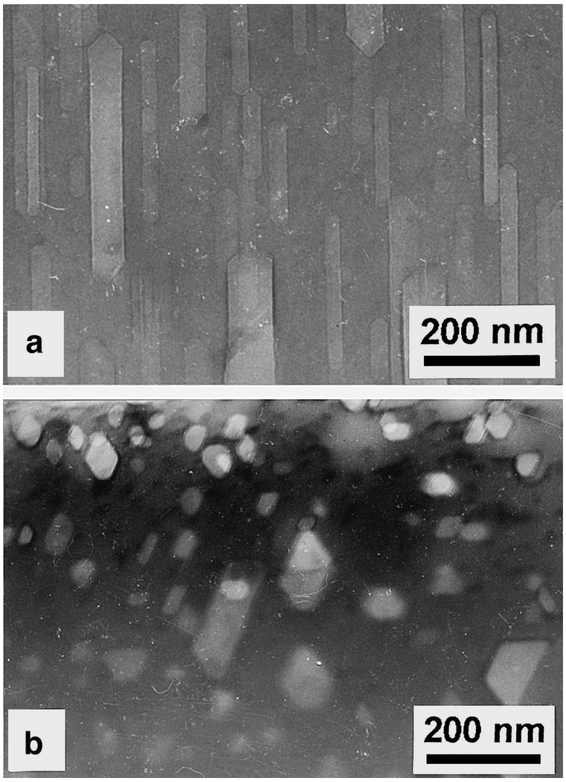

Fig. 5. Cavities in hydrogen-implanted beryllium after annealing for 15 min at 600°C. (a) Zone axis near ⟨02-21⟩, cavities are elongated along ⟨0 0 0 1⟩. (b) Zone axis ⟨0 0 0 1⟩, sidelong facets of the cavities lie along {1–100} planes.

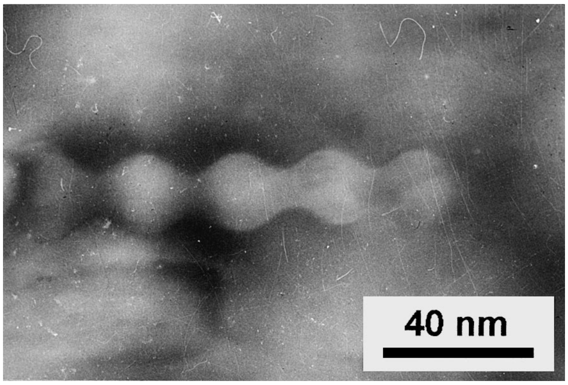

Fig. 6. TEM contrast of a cavity under dynamic imaging conditions.

plantation the hydrogen atoms are accumulated near basal planes of beryllium. This can lead at higher doses to the formation of a new crystal structure, probably in the form of platelet clusters, which has been previously observed in other metals, irradiated by low energy hydrogen isotope ions [15,16]. It is possible to suppose that the small regions with different crystal structure observed in the hydrogen-doped zone in the present study are also some kind of hydrogen-containing precipitates.

The significant difference of the present experiment from other similar works is the higher energy of incident hydrogen ions and, hence, the lower influence of the sample surface as a sink for interstitials and vacancies. Such influence takes place both under irradiation and

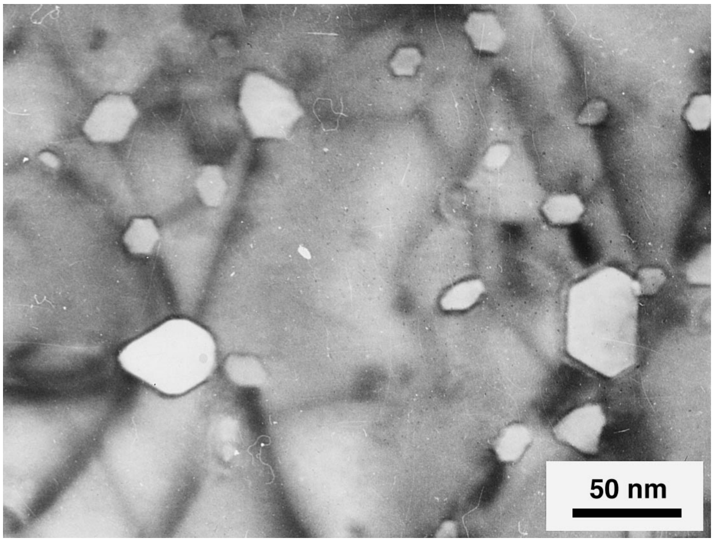

Fig. 7. Dislocations and bubbles in hydrogen-implanted beryllium after annealing for 15 min at 500°C; zone axis is ⟨0 0 0 1⟩. All bubbles are fixed on dislocations.

during post-irradiation annealing. This circumstance, apparently, has primarily affected the evolution of the defect structure and caused differences in behaviour compared to another study [8], where the oriented diffusive growth of cavities took place only under high temperature irradiation. During post-irradiation annealing the bubbles in [8] grew by migration and coalescence, and the ratio of facet dimensions was close to 1. An elongated shape and the presence of "teeth" on the sidelong facets of all cavities grown in our experiment testifies to the diffusion growth mechanism. The regularity and almost constant size of "teeth" are caused by the competing influence of gas pressure and surface tension, which define the equilibrium shape of cavities.

In conclusion, the study of beryllium implanted with hydrogen up to a concentration of about 1 at.% shows that the presence of hydrogen strongly affects the evolution of microstructure. In particular, the formation of regions with different crystal structure and long gas-filled cavities were observed. These observations can extend our understanding of the mechanisms of retention, desorption and permeability of hydrogen isotopes in beryllium.

References

[1] ITER Interim Design Report, International Thermonuclear Experimental Reactor, La Jolla, CA, USA, 12 July 1995.
[2] W. Bartels, S.J. Piet, G. Saji, L.N. Topilski, Safety Analysis Data List (SADL), Version 1.1, N.-W. Bartels (Ed.), S 81 RE 3 96-03-05 W1.1, ITER SEHD file #8.1.C-1, La Jolla, CA, USA, 15 March 1996.
[3] S.J. Piet, Specifications for "Source Term" Analyses for NSSR-1, vol. III, Radiological and Energy Source Terms, S 81 MD 55 96-03-04 W1.3, ITER SEHD file #8.1.C-1, La Jolla, CA, USA, 15 March 1996.
[4] V. Barabash, K. Dietz, G. Federici, G. Janeschitz, R. Matera, S. Tanaka, In: Fusion Technology 1994, Proc. of the 18th Symposium on Fusion Technology, Karlsruhe, 22–26 August 1994, p. 239.
[5] V.N. Chernikov, V.Kh. Alimov, A.P. Zakharov, in: Proc. of 2nd IEA Intern. Workshop on Beryllium Technology for Fusion, Jackson Lake Lodge, 6–8 September 1995, p. 294.
[6] D.V. Andreev, V.N. Bespalov, A.Ju. Birjukov, B.A. Gurovich, P.A. Platonov, J. Nucl. Mater. 233–237 (1996) 880.
[7] V.N. Chernikov, V.Kh. Alimov, A.V. Markin, A.E. Gorodetsky, S.L. Kanashenko, A.P. Zakharov, I.V. Kupriyanov, J. Nucl. Mater. 233–237 (1996) 860.
[8] N. Yoshida, S. Mizusawa, R. Sakamoto, T. Muroga, J. Nucl. Mater. 233–237 (1996) 874.
[9] B. Tsuchiya, K. Morita, J. Nucl. Mater. 233–237 (1996) 898.
[10] K.L. Wilson, R.A. Causey, W.L. Hsu, B.E. Mills, M.F. Smith, J.B. Whitley, J. Vac. Sci. Technol. A8 (1990) 1750.
[11] W.R. Wampler, J. Nucl. Mater. 196–198 (1992) 981.
[12] P.B. Johnson, D.J. Mazey, J.H. Evans, Rad. Effects 78 (1983) 147.
[13] R. Vianden, E.F. Kaufmann, J.W. Rodgers, Phys. Rev. 22 (1980) 63.
[14] A.E. Pontau, K.L. Wilson, F. Greulich, L.G. Haggmark, J. Nucl. Mater. 91 (1980) 343.
[15] T. Muroga, R. Sakamoto, M. Fukui, N. Yoshida, T. Tsukamoto, J. Nucl. Mater. 196–198 (1992) 1013.
[16] N. Yoshida, N. Ashizuka, T. Fujiwara, T. Kurita, T. Muroga, J. Nucl. Mater. 155–157 (1998) 775.